

Low-energy-electron-diffraction fine structure in W(001) for energies from 0 to 35 eV

J.-M. Baribeau* and J.-D. Carette†

Département de Physique, Faculté des Sciences et de Génie, Université Laval, Québec, Canada G1K 7P4

P. J. Jennings

School of Mathematical and Physical Sciences, Murdoch University, Murdoch, Western Australia, 6150, Australia

R. O. Jones

Institut für Festkörperforschung der Kernforschungsanlage Jülich, D-5170 Jülich, Federal Republic of Germany

(Received 24 June 1985)

Low-energy-electron-diffraction (LEED) intensities from the W(001) surface have been measured for incident energies from 0 to 35 eV, azimuthal angle $\phi=0^\circ$, and incident angles between 45° and 70° , with particular reference to the fine structure at very low energies. The results have been compared with calculations using a model of the surface barrier described earlier. The experimental curves can be reproduced satisfactorily, provided that (1) the inner potential is allowed to vary with incident energy, (2) the surface damping is strong and energy dependent, and (3) there is a weak dependence of the surface barrier on incident angle.

I. INTRODUCTION

The nature of the interaction between a charged particle and a surface is an important aspect of several spectroscopies. Information about the interaction in the immediate neighborhood of a surface, often referred to as the surface barrier, is of particular interest and can be studied in most detail using high-resolution low-energy electron diffraction (LEED). The origin of the fine structure, which was first observed by Adnot and Carette¹ for the W(001) surface, lies in the backscattering of the nonspecular beams by the surface barrier and their recombination with the beam specularly reflected from the surface.

There have been numerous models of the surface barrier described over the past forty years.² Based on the results of self-consistent density-functional calculations for a W(001) film, Jones *et al.*² suggested a model barrier of the form

$$V(z) = \begin{cases} \{1 - \exp[\lambda(z - z_0)]\} / [2(z - z_0)], & z < z_0 \\ -U_0 / \{A \exp[-B(z - z_0)] + 1\}, & z \geq z_0 \end{cases} \quad (1)$$

where A and B are constants determined by matching $V(z)$ and its normal derivative at the image plane z_0 , yielding $A = -1 + 2U_0/\lambda$ and $B = U_0/A$. Far from the surface the potential has the image form (relative to z_0) and it has a smooth transition to the bulk inner potential U_0 . The value of the potential at the image plane, $V(z_0)$, is equal to $-\lambda/2$. In the transition region between bulk and vacuum, the potential with the form (1) and the parameters $z_0 = 2.9$ a.u. and $\lambda = 1.1$ a.u.⁻¹ provides a satisfactory description of the parallel average of the potential of the film calculations.²

The potential resulting from the density-functional calculations is appropriate for occupied states below the Fermi energy. The optimum values of the potential parameters will differ for incident electrons with energies above

the vacuum level, and these parameters can be found by careful comparison of calculated and measured LEED fine structure. In the case of the W(001) surface and an incident angle θ of 48° , it was found that all features of the measured fine structure¹ could be reproduced accurately using a barrier of the form (1) with barrier parameters $U_0 = 1.0$ Ry and (z_0, λ) in a narrow range between $(-2.6$ a.u., 1.1 a.u.⁻¹) and $(-3.3, 0.7)$. The broad peak with maximum near 3.5 eV is reproduced best by a barrier near the edge of this range $(-3.2, 0.8)$. This model barrier also provides a satisfactory description of the striking asymmetry in the spin-up and spin-down channels in spin-polarized diffracted intensities for $15^\circ \leq \theta \leq 26^\circ$ and for energies below 10 eV.³ For these incident angles and energies, there is a delicate interaction between Bragg peaks, spin-dependent features, and barrier-scattering effects.²

Over the above restricted angle and energy ranges, there is little evidence of dynamical effects, i.e., a dependence of the electron-surface interaction on the incident velocity. A simple physical picture based on the interaction of the particle with its moving image⁴ suggests that these effects should be more pronounced for higher incident energies. For a given incident energy, they should also be more important for smaller angles of incidence.⁴ Although this picture is physically plausible, there has been no unambiguous identification of angle-dependent effects to date. Of particular interest in the present work is the energy dependence of the inner potential. Variation of U_0 with incident-beam energy can be expected, since the inner potential is the real part of the self-energy, and electron-gas calculations⁵ indicate that this quantity should decrease in magnitude as the energy increases. Ignatiev *et al.*⁶ and Clark⁷ showed that a decrease of U_0 by about 2 eV for incident energies between 20 and 150 eV improved the agreement between theory and experiment for Mo(001). LEED analyses for Cu(001) and Ni(001) (Ref.

8) also showed that the variation in U_0 for incident energies 0–40 eV was approximately 2 and 3 eV, respectively. In the case of W(001), Clarke and Morales de la Garza⁹ showed that a reduction in U_0 with increasing energy resulted in improved agreement between theory and experiment. However, the variation in inner potential proposed for energies below 40 eV was negligible.

In this paper we describe high-resolution measurements of diffracted intensities from W(001) between 2 and 6 eV, and in the range 0–35 eV for incident angles between 45° and 70° and azimuthal angle $\phi=0^\circ$. The results are compared with spin-polarized LEED intensity calculations. In Sec. II we outline the experimental technique used. In Sec. III we discuss the method of calculation and compare calculated and measured diffracted intensities. The results and their consequences are discussed in Sec. IV and our concluding remarks are given in Sec. V.

II. EXPERIMENTAL

The intensities of electrons specularly reflected from W(001) were measured with the apparatus used in previous experiments of the same kind.^{10,11} Monoenergetic electrons [15 meV full width at half maximum (FWHM)] are produced and analyzed by two identical 127° cylindrical electron spectrometers. Both are equipped with a three-element electrostatic lens which focuses the electron beam on the target. Design details can be found elsewhere.¹²

Curves of reflected current against incident energy were obtained by tuning the spectrometer to a fixed energy while sweeping the voltage applied to the crystal, the sample support, and the collimation slits at the exit and entrance of the monochromator and analyzer. This method is similar to those used by Edwards and Probst¹³ and by Adnot.¹⁴ Measurements of the current flowing through the crystal sample showed that the method provides a uniform incident-electron current of about 10^{-10} A for energies above 2 eV. Below this value, the incident current drops and spurious reflections often take place, resulting in peak positions which are less reliable than those at higher energies. This is an important consideration for θ values near and above 60°. Measurements of the current flowing through the analyzer collimation slit were also carried out. The absolute elastic reflectivities could be estimated from these to be between 5% and 10% at 5 eV and $\theta=50^\circ$. Current at the entrance slit was too weak to be detected, and it was not possible to measure the analyzer transmission function.

I - V curves were recorded in the (2–6)- and (0–35)-eV energy ranges. When studying reflectivity fine structures in the lower-energy range, the best fringe contrast was obtained using an electron beam with a large angular width (5°). However, this was found to reduce greatly the electron transmission at high energy and best results were obtained in the extended energy range with a better focused beam. Although the general line shape of the (0–35)-eV spectra was recovered from one experimental run to the other, the relative peak heights of several spectral features located below and above 5 eV were found to be sensitive to the spectrometer settings. For energies below 3 eV, the

electron beams are very sensitive to stray electromagnetic fields and other inhomogeneities, resulting in an angular spreading of the beam. Results presented here were obtained with settings for which published experimental results^{13,14} were best reproduced.

All measurements were performed in ultrahigh vacuum (UHV) at a base pressure of better than 5×10^{-11} Torr. The W(001) crystal was aligned along the azimuth $\phi=0^\circ \pm 0.5^\circ$, and details of crystal preparation can be found elsewhere.¹⁵ It should be noted that the crystal was cut at a slight angle to the (001) plane, and probably consists of a series of (001) terraces. The azimuth was chosen so that these terraces were aligned parallel to the plane of incidence. As we discuss below (Sec. IV), the overall resolution of the apparatus is a maximum for fine structure corresponding to emergent beams in this plane. During the experiments the sample was cleaned by flashing above 2400 K. Frequent oxygen annealings (a few minutes at 1500 K in 5×10^{-8} Torr O_2) were also performed for cleaning purposes. The same experimental method was used by Baribeau *et al.*¹⁶ to measure the diffracted intensities from W(110) between 0 and 30 eV for $\theta=30^\circ$, 45° , and 75° , and for W(001) at low energies. These measurements were analyzed using a model barrier similar to (1), but with a layer-dependent inner potential.

III. METHOD OF CALCULATION AND COMPARISON WITH EXPERIMENT

A. Calculation of spin-polarized diffracted intensities

The method used to calculate the diffracted electron intensities is described in detail in Ref. 17. We assume an ideal unreconstructed W(001) substrate. Backscattering-channeling experiments using high-energy ions indicate, in fact, a contraction of the outermost interlayer spacing of less than 6%,¹⁸ and recent density-functional calculations of total-energy variations yield a value of 5.7%,¹⁹ with numerically smaller expansions for the next two layers. Our experience in previous calculations indicates that fine-structure effects are insensitive to small changes in the interlayer spacing at the surface. The scattering properties of the semi-infinite crystal are then described by the layer multiple-scattering method, which leads to the total-amplitude-reflection matrix

$$\mathbf{R}_T^{-+} = \mathbf{r}^{-+} + \mathbf{t}^{--} \mathbf{R}^{-+} (\mathbf{1} - \mathbf{r}^{++} \mathbf{R}^{-+})^{-1} \mathbf{t}^{++}. \quad (2)$$

The substrate-reflection matrix \mathbf{R} is determined as described in Ref. 17, \mathbf{r} and \mathbf{t} are reflection and transmission matrices for the surface barrier, and \mathbf{r}^{-+} , for example, denotes the scattering of an electron moving in the direction $z > 0$ into the $z < 0$ direction. The matrices \mathbf{r} and \mathbf{t} are found by integrating into the bulk, but the *phases* depend on the position of the barrier z_0 . The presence of inelastic-scattering effects allows us to expand the matrix inverse in Eq. (2) as a series and to truncate it to include only “double-diffraction” terms.¹⁷ There may be energy ranges for which this approximation is less accurate. The scattering process is depicted in Fig. 1 for two different values of the momentum parallel to the surface, \mathbf{g}_\parallel . The interference between the specular beam and a

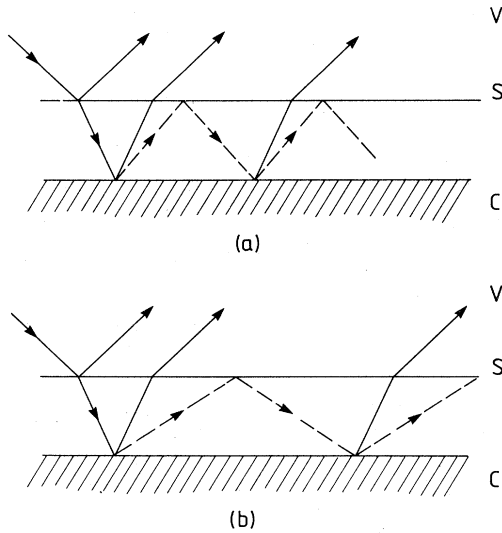


FIG. 1. Double-diffraction terms in expansion of Eq. (2) for two different values of g_{\parallel} . C denotes the crystal, S the surface barrier, and V the vacuum region.

nonspecular beam which has undergone backscattering by the surface barrier is apparent. As noted above, this mechanism is responsible for the fine structure. For spin-polarized LEED with N diffracted beams, the matrices in Eq. (2) have the dimensions $2N \times 2N$, and we use $N=20$ and phase shifts up to $l_{\max}=4$ in the present calculations. These should be adequate for incident energies below 35 eV, although caution is necessary for angles approaching grazing incidence. Thermal-diffuse-scattering effects are neglected. It is important to note¹⁷ that some features present in non-spin-polarized measurements can be traced to the effects of spin, and cannot be reproduced by calculations which neglect them.

It is well known that inelastic-scattering processes play an essential role in determining LEED intensities. In the present work, we use an energy-dependent bulk damping of the form suggested by McRae and Caldwell²⁰ on the basis of electron-reflectivity measurements on transition metals,

$$V_{\text{im}}^{\text{bulk}}(E) = V_0 \left[1 + \frac{E}{\Phi} \right]^{1.7}, \quad (3)$$

where $\Phi=5$ eV and we use the value $V_0=0.1$ Ry. The formula (3) increases monotonically with energy, and we have used an upper cutoff for $V_{\text{im}}^{\text{bulk}}$ of 3 eV. There will also be damping associated with inelastic processes at the surface, and we use an imaginary part of the surface barrier of the form

$$V_{\text{im}} = \alpha V_{\text{im}}^{\text{bulk}}(E) \exp(-\beta |z|). \quad (4)$$

This is proportional to the bulk damping [Eq. (3)], is centered on the outermost atomic plane, and decays exponentially into both bulk and vacuum regions. In Ref. 2 we adopted the values $\alpha=1$ and $\beta=0.2$ a.u.⁻¹ throughout. The absolute values of the calculated reflectivities are changed if we use different forms of V_{im} and $V_{\text{im}}^{\text{bulk}}$, but

the overall shapes of the profiles are very similar. As a point of detail, we note that evanescent beams are included in the reflection matrix only within a given energy range (typically 0.3–0.5 Ry) of their emergence from the crystal.

B. Comparison between theory and experiment

The model barrier of the form (1) is one dimensional and neglects potential variations parallel to the surface of the type apparent in Fig. 4 of Ref. 2. Even with this simplification, it is impracticable to optimize the parameters U_0 , z_0 , and λ (which may be energy and angle dependent), as well as the parameters which describe the bulk and surface inelastic effects and the departures of the ion-scattering potential from the muffin-tin form. In earlier work² the aim was to find the barrier of the form (1) which gave the best overall fit to the measured intensities for incident energies below 10 eV and a limited range of incident angles. The wider range of the present data means that it is essential also to consider the dependence on energy and angle. The connection between $U_0(z_0)$ and λ noted above implies a related energy dependence of $U_0(E)$ and $\lambda(E)$. We have assumed this in the present work, i.e.,

$$\lambda(E) = U_0(E)\lambda(0)/U_0(0). \quad (5)$$

To compare the calculated and measured intensities, we have proceeded as follows: (1) For a given angle of incidence, we have used the optimal parameters found for $\theta=48^\circ$ and determined U_0 as a function of E from the calculated Bragg peak positions. The dependence is approximately linear, from 1.05 Ry at zero incident energy to $U_0=0.88$ Ry at $E=35$ eV. (2) The high-resolution data (2–6 eV) is then studied to optimize the values of z_0 and λ for each value of θ . A small uncertainty in the incident energy (0–100 meV) is allowed for by aligning the threshold energies. The emphasis here is then on the energy intervals between the different maxima and minima. (3) The sensitivity of measured threshold features to the parameters defining the damping is then tested, and the above steps repeated as necessary.

In Fig. 2 we show the measured and calculated intensities for the high-resolution data ($2 \leq E \leq 6$ eV). The interval between calculated energy points over the region of the fine structure was 10 meV. The value of U_0 varies little for incident energies in this range and we find that a value of $U_0(0)=1.05$ Ry gives a slight improvement over the value used in Refs. 2 and 17. We show calculated intensities for both spin-up and spin-down incident beams. For these energies and angles, the calculated asymmetry between up and down channels is relatively weak, but there are differences in the positions of the peaks and minima of up to 0.1 eV. The comparison with experiment has been carried out using the average of the spin-up and spin-down intensities. As in Ref. 2, we find that the fine structure for a given angle of incidence can be reproduced to within the experimental resolution by a narrow valley of barriers in (z_0, λ) space of the form (1). Further information is provided by the position and shape of the first peak but, as noted above, these are rather sensitive to ex-

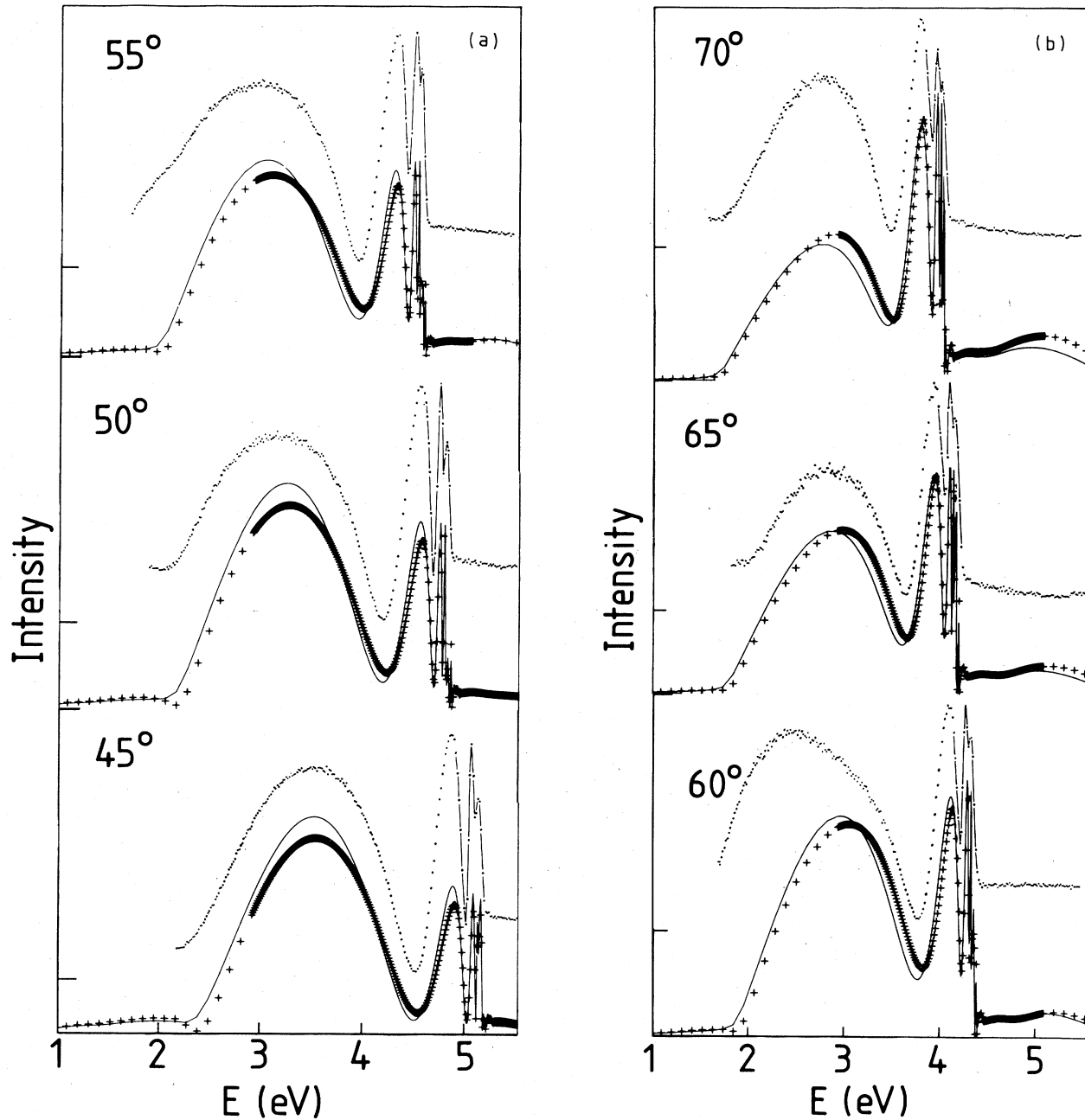


FIG. 2. Measured and calculated diffracted intensities for incident energies between 2 and 6 eV. (a) $\theta=45^\circ$, 50° , and 55° . (b) $\theta=60^\circ$, 65° , and 70° . The calculated intensities are for spin-up (pluses) and spin-down (solid curve) electrons. The energy interval in the calculations is 0.01 eV.

perimental conditions, particularly for angles of incidence of 60° and above. Inclusion of this peak, where appropriate, leads to a barrier which reproduces the positions of all resolved maxima and minima in this energy range. There is a weak variation of the optimum barrier form from (2.9, 0.75) to (3.0, 0.92) as θ from 45° to 70° . The corresponding curves are shown in Fig. 2 and we return to this point in Sec. IV.

For incident energies below 6 eV, the energy-dependent V_{im}^{bulk} is small, and different choices of surface-damping

parameters α and β [Eq. (4)] produce minor changes in the calculated fine structure. This is not true for the extended range 0–35 eV. In Fig. 3 we compare the measured curve for $\theta=45^\circ$ with the average of the spin-up and spin-down calculations using $\beta=0.2 \text{ a.u.}^{-1}$ and values of α between 0 and 2. Analogous results are obtained if α is held fixed and β , i.e., the spatial extent of the surface damping, is varied. Two effects are striking. (i) The reflectivities are lowered substantially (approximately halved) when α is increased in this range, i.e., even

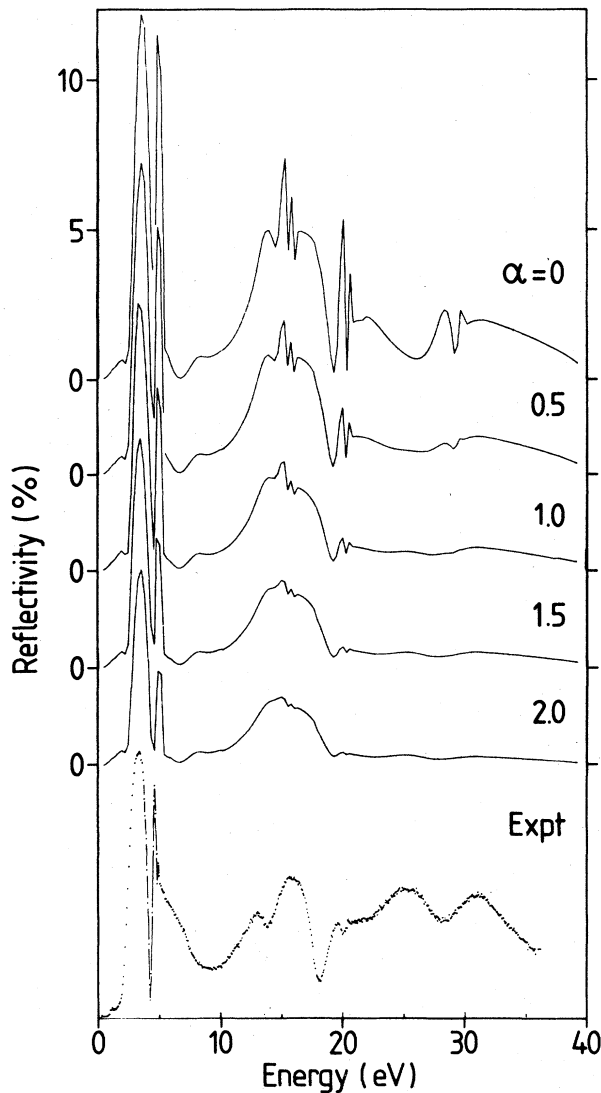


FIG. 3. (a) Measured intensities and (b) spin-averaged calculated intensities for $\theta=45^\circ$ for different surface damping parameters α . The calculated reflectivities are on the same scale. The energy interval in the calculations is 0.25 eV.

with a fixed bulk damping, the reflectivity is remarkably sensitive to the details of the surface inelastic processes. (ii) Consistent with the interference origin of the threshold effects, there is a pronounced reduction in the fine structure as α increases. This correlation of fine structure with the strength of the barrier damping is of particular interest, since the experimental curve in Fig. 3 shows no measurable threshold effects for energies above about 20 eV. For the remainder of the calculations presented here, we use the values $\alpha=1.0$, $\beta=0.2$.

In Fig. 4(a) we show the measured spectra for incident energies 0–35 eV for $45^\circ < \theta < 70^\circ$. Figure 4(b) shows the corresponding calculations for spin-up and spin-down electrons using the barrier parameters optimized for each angle as described above. The reflectivity is given in arbitrary units. The calculations indicate, however, that the

reflectivity is an order of magnitude higher for $\theta=45^\circ$ than for $\theta=70^\circ$. The overall agreement between theory and experiment is satisfactory, although the calculations show pronounced minima above the first threshold which are not evident in the measurements. The differences between spin-up and spin-down intensities show that spin-orbit effects are substantial, in contrast to the assumption of Le Bosse *et al.*²¹ In this energy range a constant value of the inner potential leads to an unsatisfactory description of peak positions. As noted above, we find that U_0 decreases smoothly by about 2 eV over this energy range, a similar behavior to that found by Jennings and Thurgate⁸ in Ni and Cu. It should be noted that the Bragg-peak positions depend weakly on the form of the damping assumed.

IV. DISCUSSION

The analysis of LEED intensity measurements is complicated by the number of physical processes which can affect them. The scattering potential of the bulk, the details of the barrier potential, and bulk- and surface-damping processes all enter in important ways. In view of the number of parameters which may be used, it is important to focus on those experimental features which are as sensitive to as few as possible. In this paper, we study two in particular: (1) the fine structure at low energies and its disappearance at energies above 20 eV, and (2) the energy dependence of the inner potential. We have seen in the preceding section that the form of the latter is consistent with that found in earlier work.⁸

The fine structure at low energies provides a sensitive probe of the shape of the surface barrier, and its energy dependence is particularly interesting. Figure 1 shows that the fine structures associated with larger values of $|\mathbf{k}_\parallel + \mathbf{g}_\parallel|$ require coherent scattering and therefore an essentially perfect surface over a greater range. For $\theta=45^\circ$ and azimuthal angle $\phi=0^\circ$, for example, threshold effects are evident in the calculations near 5 eV [$\mathbf{g}_\parallel=(\bar{1}0)$], 16 eV [$(\bar{1}\bar{1})$, $(\bar{1}1)$], 26 eV [$(\bar{2}0)$], and 30 eV [$(\bar{2}\bar{1})$, $(\bar{2}1)$, $(0\bar{1})$, (01)]. The experimental results (Fig. 3) show clear threshold structures associated with both the $(\bar{1}0)$ and $(\bar{2}0)$ emergences, but none which can be related unambiguously to the others. This indication that the registry is best in the $(\bar{1}0)$ direction is consistent with the fact that the crystal was cut slightly off the (001) surface, resulting in a series of (001) terraces (see Sec. II above). The sensitivity of the fine structure to surface imperfections is consistent with our findings that these features differ for different crystals.

The energy dependence of the fine structure and a correlation with the emergent beams can then yield information about the degree of perfection of the surface. Measurements of surface roughness are important, but difficult to carry out.²² In principle, the parameters α and β in Eq. (4) could be associated with surface damping and the depth of surface disorder, respectively, but the present results do not allow a clear separation to be made. A discussion of the effects of chemisorption on the fine structure has been given by Thurgate and Jennings.²³

Although the disappearance of threshold features at higher energies is consistent with increased damping, ex-

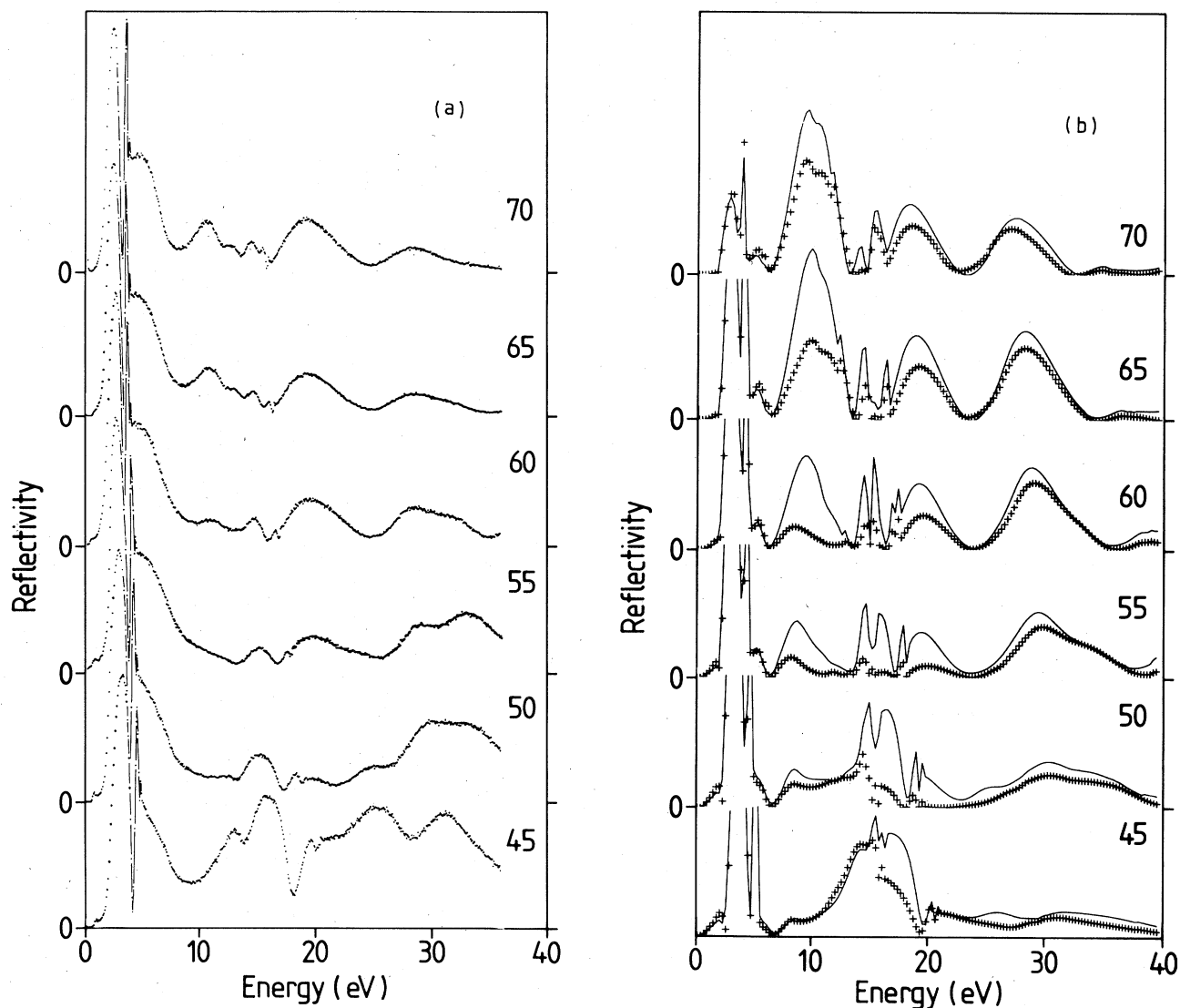


FIG. 4. (a) Measured and (b) calculated spin-polarized intensities (both in arbitrary units) for $45^\circ \leq \theta \leq 70^\circ$ and energies from 0 to 35 eV. For the calculated curves, pluses and solid curves denote spin-up and spin-down intensities, respectively. The energy interval in the calculations is 0.25 eV.

perimental uncertainties certainly play an important role. Gaubert *et al.*²⁴ showed recently that the angular dispersion of the incident beam is crucial in determining the experimental resolution. Furthermore, they showed that the optimum resolution of fine structure is obtained where the emergent beams are antiparallel to the incident direction, and that an azimuthal accuracy of 0.1° would be necessary to obtain an overall resolution of ~ 10 meV. Since this is not currently attainable, either in the present apparatus or elsewhere, fine structure arising from pre-emergent beams far from the plane of incidence will be much reduced.

We have noted that the optimum barrier of the form (1) changes as the angle of incidence varies between 45° and 70° , the main effect being a slight increase in λ with increasing θ . The actual angular dependence of the potential experienced by the incident electron is difficult to ex-

tract, however, since the mechanism leading to fine structure (Fig. 1) involves emergent beams moving almost parallel to the surface. It is nevertheless interesting to discuss two possible effects which could contribute, dynamical effects and the three-dimensional nature of the barrier.

In the model calculation of Harris and Jones,⁴ the velocity-dependent contribution to the force has a parallel component which is half the normal component, i.e., the velocity-dependent corrections become smaller for larger angles of incidence. This is in qualitative agreement with the observed behavior. The effect of the three-dimensional variation in the potential can be examined in terms of a simple model used by Garcia²⁴ to study the effect of surface corrugation on image-potential surface states. In this model the potential variation parallel to the surface is described by a single Fourier component. This is z dependent, of course, and so has a greater effect on

fine-structure features farthest from threshold. The displacement in the energy which results is greatest for smaller angles of incidence,²⁶ qualitatively the same feature as observed. However, the self-consistent density-functional calculations of the surface potential for W(001) (Ref. 2) give Fourier components which are small. This effect will therefore be small, and the low energy of the incident electrons means that dynamical effects will also be very small. Furthermore, uncertainties in both the measurements (angular resolution, etc.) and the calculations (convergence of phase-shift and beam expansions) could lead to apparent angle-dependent effects. As a result, no definite statement about such effects is possible.

V. CONCLUDING REMARKS

High-resolution LEED intensity measurements provide the most promising source of information about the surface potential barrier and a useful complement to other techniques for surface-structure determination. In the present work we have analyzed measurements on W(001) for $\phi=0^\circ$, energies in the range 0–35 eV, and incident angles between 45° and 70° . Our main conclusions are the following:

(i) The fine structure for incident energies below 6 eV can be reproduced extremely well by a one-dimensional barrier model. The location of the image plane relative to the outermost atomic plane is very similar to that found in density-functional calculations for the W(001) surface ($z_0 \sim 2.9$ a.u.). The evidence for an angular dependence of the barrier is weak and cannot be considered conclusive.

(ii) The measured intensities for incident energies out to 35 eV are reproduced satisfactorily, provided that the inner potential is energy dependent. Although experimental uncertainties in the azimuthal angle will also contribute, the damping of the threshold features for energies above 20 eV is consistent with a strong and energy-dependent surface damping.

(iii) Spin-polarization effects are important, particularly for incident energies above the first threshold.

It is important to note that a complete optimization of the parameters describing the surface structure and the surface potential is impracticable, so that the optimum form of the surface barrier will depend to some extent on other input parameters which are not optimized. This may account for the different barriers found here and in Ref. 16. Accurate estimates of the absolute reflectivities would aid in discriminating between different models.

*Present address: Division of Microstructural Sciences, National Research Council of Canada, Ottawa, Canada K1A 0R6.

†Deceased.

¹A. Adnot and J.-D. Carette, Phys. Rev. Lett. **38**, 1084 (1977).

²R. O. Jones, P. J. Jennings, and O. Jepsen, Phys. Rev. B **29**, 6474 (1984). This paper includes a survey of earlier barrier models.

³E. G. McRae, D. T. Pierce, G.-C. Wang, and R. J. Celotta, Phys. Rev. B **24**, 4230 (1981).

⁴J. Harris and R. O. Jones, J. Phys. C **6**, 3585 (1973); **7**, 3751 (1974).

⁵L. Hedin and B. I. Lundqvist, J. Phys. C **4**, 2064 (1971).

⁶A. Ignatiev, F. Jona, H. D. Shih, D. W. Jepsen, and P. M. Marcus, Phys. Rev. B **11**, 4787 (1975).

⁷L. J. Clarke, Surf. Sci. **91**, 131 (1980).

⁸P. J. Jennings and S. M. Thurgate, Surf. Sci. **104**, L210 (1981).

See also D. W. Jepsen, P. M. Marcus, and F. Jona, Phys. Rev. B **5**, 3933 (1972) [Ni(001), 50–200 eV]; S. Å. Lindgren, L. Wallden, J. Rundgren, and P. Westrin, Phys. Rev. Lett. **50**, 368 (1983) [Cu(001), 20–120 eV].

⁹L. J. Clarke and L. Morales de la Garza, Surf. Sci. **99**, 419 (1980).

¹⁰J.-M. Baribeau and J.-D. Carette, Phys. Rev. B **23**, 6207 (1981).

¹¹J.-M. Baribeau and J.-D. Carette, Surf. Sci. **112**, 241 (1981).

¹²D. Roy and J.-D. Carette, in *Electron Spectroscopy for Surface Analysis*, Vol. 4 of *Topics of Current Physics*, edited by H. Ibach (Springer, Berlin, 1977), p. 13.

¹³D. Edwards and F. M. Propst, J. Chem. Phys. **56**, 3184 (1972).

¹⁴A. Adnot, Ph.D. thesis, Université Laval, 1977.

¹⁵J.-M. Baribeau and J.-D. Carette, Surf. Sci. **134**, 886 (1983).

¹⁶J.-M. Baribeau, J. C. Le Bosse, and J. Lopez, J. Phys. C **18**, L73 (1985); J. Lopez, J. C. Le Bosse, and J.-M. Baribeau, *ibid.* **18**, 2197 (1985); J.-M. Baribeau, J. Lopez, and J. C. Le Bosse,

ibid. **18**, 3083 (1985).

¹⁷R. O. Jones and P. J. Jennings, Phys. Rev. B **27**, 4702 (1983).

¹⁸L. C. Feldman, R. L. Kauffmann, P. J. Silverman, R. A. Zuhr, and J. H. Barrett, Phys. Rev. Lett. **39**, 38 (1977).

¹⁹C. L. Fu, S. Ohnishi, E. Wimmer, and A. J. Freeman, Phys. Rev. Lett. **53**, 675 (1984).

²⁰E. G. McRae and C. W. Caldwell, Surf. Sci. **57**, 766 (1976).

²¹J. C. Le Bosse, J. Lopez, J.-M. Baribeau, and J.-D. Carette, Surf. Sci. **137**, 361 (1984).

²²One measure of surface roughness (or diffusivity) is the ratio of specular reflectivity to the total elastic reflectivity at very low energies. A rather precise estimate of the surface roughness of a liquid-vapor interface for pure water was given by the x-ray reflectivity measurements of A. Braslau, M. Deutsch, P. S. Pershan, A. H. Weiss, J. Als-Nielsen, and J. Bohr [Phys. Rev. Lett. **54**, 114 (1985)]. A direct method of determining surface structure, such as the scanning tunneling electron microscope, could provide information about the local disorder. For an application of this technique to surface structure, see G. Binnig, H. Rohrer, C. Gerber, and E. Weibel, Phys. Rev. Lett. **50**, 120 (1983).

²³S. M. Thurgate and P. J. Jennings, Appl. Surf. Sci. **22/23**, 478 (1985).

²⁴C. Gaubert, R. Baudoing, Y. Gauthier, and J. Rundgren, Surf. Sci. **147**, 162 (1985).

²⁵N. Garcia, B. Reihl, K. H. Frank, and A. R. Williams, Phys. Rev. Lett. **54**, 591 (1985).

²⁶For a one-dimensional barrier, energies of the threshold features depend only on the component of the momentum, k_z , normal to the surface. For constant incident energy $\sim(k_z^2 + k_{\parallel}^2)$, the threshold peaks move closer to the emergence energy as θ increases. The corresponding wave functions become increasingly extended and the influence of the corrugation potential progressively weaker.